

Observation of surface polarity dependent phonons in SiC by deep ultraviolet Raman spectroscopy

S. Nakashima,¹ T. Mitani,¹ T. Tomita,² T. Kato,¹ S. Nishizawa,¹ H. Okumura,¹ and H. Harima³

¹National Institute of Advanced Industrial Science and Technology, Central 2, Umezono 1-1-1, Tsukuba, Ibaraki 305-8568, Japan

²Department of Ecosystem Engineering, The University of Tokushima, Tokushima 770-8506, Japan

³Department of Electronics and Information Science, Kyoto Institute of Technology, Matsugasaki, Kyoto 606-8585, Japan

(Received 13 November 2006; revised manuscript received 25 January 2007; published 23 March 2007)

Backscattering Raman spectra of SiC polytype crystals with SiC{0001} polar faces have been measured using deep ultraviolet (DUV), UV, and visible (VIS) excitation sources. We have found that for DUV excitation the intensity profiles of zone-folded modes differ markedly for Si and C faces. This Raman spectral feature is attributed to the presence of nonpropagating phonon modes confined in the near-surface region. It is concluded that the surface-bound phonon modes created with DUV photon field extend over a region a few hundred nanometers in depth, and that the displacements of the phonon modes are anisotropic in the direction of the polar axis. This surface-orientation-dependent Raman spectrum can be used to identify the surface polarity of SiC polytypes.

DOI: [10.1103/PhysRevB.75.115321](https://doi.org/10.1103/PhysRevB.75.115321)

PACS number(s): 78.30.-j, 63.20.-e, 78.68.+m

Raman scattering is sensitive to the properties of the surface layers of a sample being investigated when the penetration depth of excitation light is limited to the surface region. Recently, Raman scattering with deep ultraviolet (DUV) laser light as an excitation source has been applied to examining near surface layers of wide-gap semiconductors such as SiC and Ga_xAl_{1-x}N, because DUV Raman scattering can be used to probe shallow surface layers with thicknesses ranging from a few nanometers to hundreds of nanometers and the resonance effect enables observation of Raman signals with a high signal-to-noise ratio.¹ It is expected that DUV Raman scattering provides information upon force-field structure and phonon states in a near-surface region.

Surface phonon modes have been studied both theoretically and experimentally for a long time. The surface-localized modes in finite slabs and semi-infinite lattices with foreign atoms at free ends have been studied using one-dimensional models.²⁻⁴ It has been proven that surface modes occur under certain conditions. The presence of surface modes that extend towards the interior of crystals has been investigated theoretically for regular crystals with free ends using one-, two-, and three-dimensional models.⁵⁻⁹ Wallis and his group^{2,3} and Hori and Asahi⁴ have examined vibrations in finite one-dimensional diatomic lattices with free ends and have shown that there exist surface-localized modes of vibration with a frequency in the forbidden gap between the optical and acoustical branches. Wallis demonstrated that there are phonon modes with a wavelike character in addition to the surface localized mode which lies in the forbidden gap and decays within a few atomic layers.² The attenuation depth of the surface mode was calculated for semi-infinite rocksalt crystals by Achar and Barsch, who showed that the surface modes extend for up to 50 atomic layers.⁸

To date, surface-localized phonons in crystals have mainly been observed by high-resolution electron energy-loss spectroscopy (HREELS).¹⁰ Recently, the surface localized mode was measured by Raman scattering for adsorbate-terminated semiconductor surfaces and clean III-V semiconductor surfaces.^{11,12} However, surface Raman measurements have been limited to surface phonon modes local-

ized within a few atomic layers at the surface.

Surface-confined phonons have also been studied in GaAs-AlAs superlattices.¹³⁻¹⁵ Sorba *et al.*¹³ showed that in addition to surface modes of semi-infinite GaAs (AlAs), new surface modes appear in the extra gaps of the superlattice that decay exponentially toward the interior of the crystal. However, particular attention has been given to determination of the frequencies of the surface phonon modes, while experimental work on atomic displacements of these modes, which are closely correlated with the Raman intensity, has not well been performed so far.

In this work, we have measured DUV Raman spectral profiles of several SiC polytype crystals with {0001} faces. SiC polytypes form natural superlattices and show various zone-folded modes.¹⁶⁻¹⁹ We have found that Raman intensity profiles of the zone-folded modes in transverse and longitudinal branches differ strikingly for the Si(0001) and C(000-1) polar faces for DUV excitation. We attribute this feature to the presence of surface phonon modes bound to the near-surface region, whose displacement patterns depend on the surface orientation and also the penetration depth of the excitation radiation.

Raman microscopy measurements were carried out at room temperature with a backscattering configuration using {0001} faces of SiC polytype plates that were mirror-polished on both sides. The samples used in this experiment were undoped crystals of 4H, 6H, and 15R polytypes. The surface polarities of the samples were determined beforehand from the oxidation rates of the two surfaces. The laser light sources used were the 244-nm second harmonic of an Ar⁺ ion laser and the 266-nm fourth harmonic of a yttrium-aluminum-garnet (YAG) laser. UV lasers operating at 325 and 364 nm and visible laser lines from 514.5 to 632.8 nm were also used in some measurements. The Raman penetration depth $d_{\text{Ram}} [=1/(2\alpha)$: α is absorption coefficient] in α -SiC is ~ 100 , ~ 200 , and ~ 2000 nm at wavelengths of 244, 266, and 325 nm, respectively.²⁰

The folded modes of the transverse acoustic (FTA), longitudinal acoustic (FLA), and longitudinal optical (FLO) branches in SiC polytypes show sharp doublets for the folded

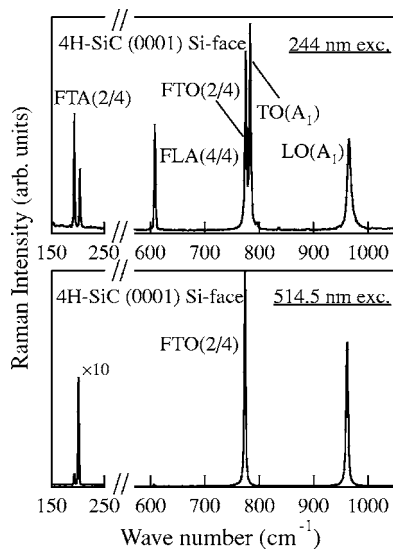


FIG. 1. Raman spectrum of 4H-SiC polytype crystal observed for 244- and 514.5-nm excitation.

modes corresponding to a phonon inside the Brillouin zone of the basic polytype (3C-SiC).^{16–19} The zone-folded modes are designated by the reduced wave vector, $x (=q/q_B)$; a folded mode corresponds to a phonon mode at a reduced wave vector in the Brillouin zone of the 3C polytype (zincblende structure).¹⁸ Doublets of the folded modes are designated as, e.g., FTA($\pm x$) and FLO($\pm x$).

In Fig. 1, we show Raman spectra obtained from the 4H-SiC crystal with Si(0001) faces for 244- and 514.5-nm excitations. For DUV excitation, a striking resonance enhancement^{1,21} was found for the Raman bands of the FTA(2/4) mode at around 200 cm^{-1} , for the FLA(4/4) mode at 610 cm^{-1} , and for the forbidden TO (A_1) band at 776 cm^{-1} . The FTA($\pm 2/4$) mode forms a doublet for which the relative intensities of the low- and high-frequency counterparts are markedly different for DUV and visible (VIS) excitations. The intensities of these folded modes are much weaker than those of the TO (E_2) and LO (A_1) modes.

Figure 2 shows DUV Raman spectra of several folded modes from the Si(0001) and C(000-1) faces measured with 244-nm excitation for 4H-, 6H-, and 15R-SiC. These folded modes consist of doublets and both the high- and low-frequency components are very sharp, being less than 2 cm^{-1} in width, although the intensities of these folded modes are much weaker than those of the TO(E_2) and LO(A_1) modes. As shown in this figure, the relative intensities of the two counterparts of the doublets are different for the opposite faces. The intensity ratios of the counterparts in the FTA($\pm 2/4$) mode are reversed for the Si and C faces.

The Raman spectral profiles of the folded modes in SiC polytypes have already been measured in detail for VIS excitation and compared with the calculated results of traveling wave solutions for atomic displacements.^{18,19} The calculated intensity ratio $I(+)/I(-)$ of the FTA(2/4) mode in the 4H polytype is about 11 for 514.5-nm excitation. The experimental intensity ratio is about 10, being in agreement with the calculated intensity ratio. For 244-nm excitation,

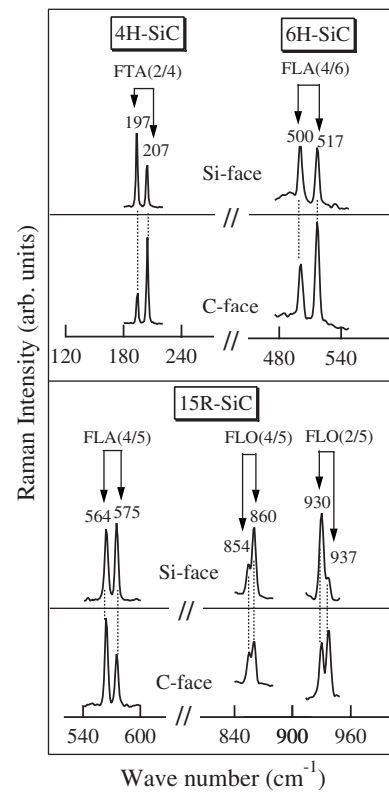


FIG. 2. The Raman intensity profiles for Si(0001) and C(000-1) faces are shown for typical folded modes in 4H-, 6H- and 15R-SiC polytypes.

$I(+)/I(-)$ is 1.84 and 0.14 for Si and C faces, respectively.

The intensity profiles of these doublets vary with the wavelength used for excitation; in other words, the optical penetration depth of the excitation light. Figure 3 shows Raman profiles of the FLA(4/5) and FLO(2/5) modes in the

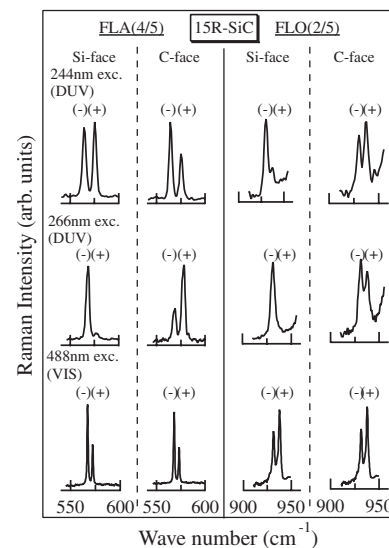


FIG. 3. Raman profiles of FLA(4/5) and FLO(2/5) modes in the 15R-SiC polytype measured for three different excitation wavelengths of 244, 266, and 488 nm. The Si-face spectra are compared with the C-face spectra.

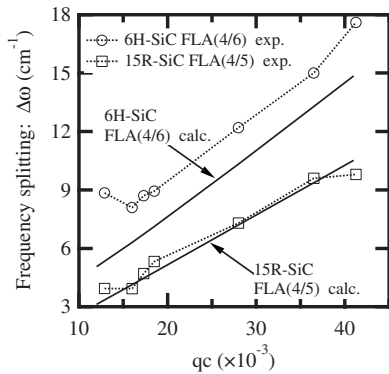


FIG. 4. Frequency splitting of the FLA(4/6) doublet in 6H-SiC and the FLA(4/5) doublet in 15R-SiC is plotted as a function of momentum transfer. c is the unit-cell length of 3C-SiC along the $\langle 111 \rangle$ direction.

15R-polytype, which were obtained from Si and C faces for three different laser lines at 244, 266, and 488 nm. The Raman intensity profiles of the doublets differed for Si and C faces when 244- and 266-nm excitation sources were used, although the peak frequencies of these folded modes are the same within experimental uncertainty ($\pm 0.5 \text{ cm}^{-1}$). In contrast, for the 488-nm light and also other UV and VIS laser lines including 632.8- and 325-nm lines, the spectral profiles and the peak frequency exhibit no surface-orientation dependence, although the intensity ratio of the counterpart of the doublets $I(+)/I(-)$ has some dependence on the excitation wavelength and hence the momentum transfer q as reported in Ref. 22.

In order to further study the nature of surface-orientation-dependent phonon modes, we have measured the frequency of these modes using various excitation lines. Figure 4 shows the frequency splitting of several doublets in the 15R and 6H polytypes as a function of momentum transfer q . In the back-scattering geometry, the momentum transfer is given by $q = 4\pi n/\lambda$ where n is refractive index of the material and λ is the wavelength of the incident light. The splitting value of the doublets increases with increasing q , as expected for the folded modes of acoustic branches in natural²² and artificial superlattices.²³ In this figure we also plot the frequency splitting calculated for traveling-wave phonon modes in bulk.^{18,19} The calculated frequency splitting for the FLA(4/6) doublet in the 6H polytype and the FLA(4/5) doublet in the 15R polytype is in agreement with experimental results for VIS and UV excitations. The experimental values for the FLA(4/6) mode in 6H-SiC deviate slightly from the calculated ones, but show a similar trend as shown in this figure. The splitting of these doublets for 244- and 266-nm excitations lie on curves calculated with the assumption of traveling-wave solutions. These results indicate that the frequencies of the DUV-excited phonon modes are very close to that of a corresponding bulk mode. This finding, together with the observation of very sharp folded modes, strongly suggests that the observed phonon modes are not the surface-localized modes with large damping that lie in the forbidden gap, even though these modes are confined in the near surface. In addition, we also have tried to observe surface local-

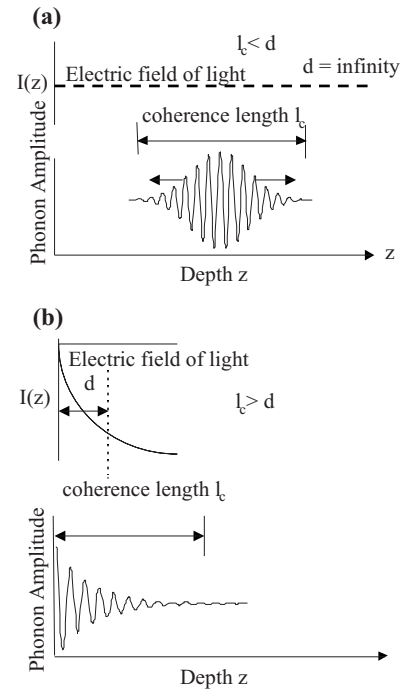


FIG. 5. Behavior of optical phonons near surfaces is classified into two categories according to its coherence length l_c and size d of the region where incident photons exist. (a) Traveling wave is formed in the case of $d > l_c$ and (b) standing wave is formed in the case of $d < l_c$.

ized modes whose frequencies lie in a forbidden gap. However, such phonon modes could not be detected, presumably because their intensity is very weak.

As shown in Figs. 2 and 3, Raman spectral profiles with marked surface polarity dependence are observed for the doublet of the folded modes. Such spectra appear only with 244- and 266-nm excitation light whose penetration depths are 100 and 200 nm, respectively. Furthermore, the spectral profiles of the doublets are different for 244- and 266-nm DUV excitations. These results may indicate that the phonon modes observed for the two excitations are stuck at the surface, being confined in a near-surface region which is comparable to an optical penetration depth of DUV light. This surface-polarity-dependent Raman spectral profile would be caused by a difference in the displacement between the standing phonon modes along the polar axes perpendicular to the Si and C terminated surfaces.

Phonon modes in solids are always damped modes, and their behavior is classified into two categories according to their coherence length. When the coherence length of the phonon modes l_c (considered to be several hundred nm or more) are larger than the penetration depth of the excitation light d as shown in Fig. 5(b), the phonon mode forms standing wave and its phase is fixed. In contrast, for visible excitation, l_c is smaller than d as shown in Fig. 5(a) and the phonon mode forms a traveling wave which is obtained under the periodic boundary condition. In this case, we observe phonon modes whose atomic displacements have various phases. Hence Raman intensity profiles obtained from the traveling-wave solutions are not significantly sensitive to the atomic arrangement in the surface layer.

In the DUV excitation case, the photon field decreases exponentially towards the interior and is restricted in the near-surface region, because of strong light absorption. The phonon modes generated by this photon field should also be confined in the near surface region and form a standing wave, because the phonon field generated by photon field cannot exceed over the exciting photon field. The confinement of the DUV excited phonon modes is analogous to that of the optical phonons in artificial superlattices such as the GaAs-AlAs system. The difference is that in the former, the confinement is caused by nonuniform distribution of the excitation photon field, but in the latter it is caused by the nonuniform dielectric property arising from heterostructure. Accordingly, the generated phonon modes form standing waves and the amplitude of the envelope of atomic displacements has a maximum at the surface as for the photon field.

The standing-wave solutions may depend strongly on the boundary conditions, which are related to mass and force field configurations near the surface. In SiC crystals further neighbor forces including second and third-neighbor forces also contribute to interatomic forces.^{17,18}

Raman intensity profiles of SiC polytypes have been calculated based on the bond polarizability concept.¹⁷⁻¹⁹ Raman scattering efficiency is related to the Raman bond polarizability and relative displacements of neighboring atoms:

$$W(\omega) \propto \left| \sum \alpha'_j (u_j - u_{j+1}) \exp(iqz) \right|^2,$$

where α'_j is the effective Raman bond polarizability for neighboring atomic planes and u_j is displacement of j th atomic plane. Weak Raman intensity for the folded modes in longitudinal and transverse acoustic branches arise from partial cancellation of the contributions from individual Raman polarizabilities.¹⁷⁻¹⁹ To qualitatively understand the observation of surface-polarity-sensitive Raman intensity profiles, we have calculated the frequencies and displacements of the surface-bound phonons, using a slab-shaped one-dimensional model of a lattice with 500 atomic layers with free ends and including third-neighbor force constants. The calculated frequency of the longitudinal modes for the slab model is almost identical to that of the corresponding bulk modes obtained under the periodic boundary condition. The calculation of the displacements shows that in addition to surface-localized modes for the C face that lie in the forbidden gap between the optical and acoustical branches, there exist standing phonon modes that extend over the entire chain, which may correspond to phonon modes with a wave-like character as studied by Wallis for finite one-dimensional lattices.² It should be noted that the displacement of the atomic planes is sensitive to both the mass and force fields at the surface layer. Taking into account the second- and third-neighbor forces in the slab model readily results in the difference in force field between the Si and C surfaces. We assumed that the displacement patterns of the standing-wave solutions for the DUV-photon-excited surface-bound phonons could be constructed with the standing-wave solution modified by an exponentially decaying function as an envelope function, since the intensity of the incident DUV light decreases exponentially in SiC surface region. We have

calculated Raman intensity profiles for Si- and C-terminated surfaces using the displacements of the surface-bound phonons thus obtained. The calculated Raman intensity profiles of the folded mode differ for Si- and C-terminated surfaces. Since the weak Raman intensities of the FTA, FLA, and FLO bands are caused by the partial cancellation of the individual bond Raman polarizabilities,^{18,19} the change in the displacement patterns leads to a marked effect on this cancellation. This would result in a change in the intensity ratio of the doublet counterparts, although the absolute intensities would not change appreciably. Furthermore, the simulation for the Raman intensity reveals that the relative intensity of doublet components changes with the decay length of the photon field, which is consistent with the change of the spectral profile observed at 266- and 244-nm excitations.

There might be another possibility that the change in the bond Raman polarizability in an ultrathin surface layer in addition to the atomic displacements would result in the variation of the Raman intensity profile. However, since the change in the bond Raman polarizability would be restricted to just a few atomic layers at the surface, the effect of this on Raman spectral intensity profiles should be small. This assumption is also confirmed by the observation that surface oxidation does not affect the spectral profiles. It should be noted that in the model analysis of the Raman intensity profile, the incorporation of further neighbor force constants than the nearest-neighbor force is necessary to explain the surface-polarity-dependent Raman profiles. A further plausible explanation for anisotropic phonon Raman spectra of Si and C faces would be presence of Fröhlich surface modes which are of the dielectric origin and appear in a frequency region between TO and LO modes.²⁴ For SiC, some of the phonons, which are infrared inactive E_2 modes and lie below TO mode, also show the surface polarity dependence. For these modes the observation of the Fröhlich surface mode could not be expected. Orientationally anisotropic Raman spectra have been observed for III-V semiconductors under resonant Raman condition.^{25,26} This anisotropy occurs for the LO phonon modes within the same face. However, for SiC, the anisotropy is found for Si and C polar faces. In this case we should consider that such interference effect occurs independently for the Si and C polar faces. It is not clear at present whether phonon modes other than the LO mode show such interference effects or not. Further theoretical study will be needed to understand the surface-polarity dependent Raman spectra of SiC crystals.

Surface-polarity-dependent Raman spectra for the folded modes may provide a technique for identifying the polarity of a {0001} SiC surface. The surface polarity of polar crystals has been identified experimentally by various methods to date.²⁷⁻²⁹ Typical methods include determination on the basis of etch pit patterns for the different surface polarities,²⁷ different oxidation rates of the opposite surfaces,²⁸ and differences in the x-ray photoelectron diffraction intensity.²⁹ Among these techniques, DUV Raman spectroscopy is a simple and useful method for determining the surface polarity of {0001} SiC nondestructively.

In conclusion, we have observed surface-orientation-dependent DUV Raman spectra for the {0001} face of α -SiC polytypes. The Raman intensity profiles of the folded modes

differ markedly for different surface polarities. This interesting finding indicates that this surface-bound phonon is directionally anisotropic along the polar axis. The observation of the anisotropic Raman spectral features is attributed to the generation of surface-orientation-sensitive phonons which are bound in the near-surface region and extend into the lattice by several hundred nanometers. These surface bound phonons are created only when the incident photon field is

limited in a shallow surface region. The Raman measurement using DUV light and the folded modes as a monitor enable us to nondestructively identify the surface polarity of SiC polytype crystals. When one uses DUV light with more short penetration depths, the study of thinner surface layers will be possible, and the DUV Raman measurements will provide us with a simple way for studying the dielectric and lattice dynamical properties in SiC surface layers.

-
- ¹S. Nakashima, H. Okumura, T. Yamamoto, and R. Shimidzu, *Appl. Spectrosc.* **58**, 224 (2004).
²R. F. Wallis, *Phys. Rev.* **105**, 540 (1957).
³R. F. Wallis, *Surf. Sci.* **2**, 146 (1964).
⁴J. Hori and T. Asahi, *Prog. Theor. Phys.* **31**, 49 (1964).
⁵R. F. Wallis, *Phys. Rev.* **116**, 302 (1959).
⁶D. C. Gazis and R. F. Wallis, *J. Math. Phys.* **3**, 190 (1962).
⁷S. Takeno, *Prog. Theor. Phys.* **30**, 1 (1963).
⁸B. N. N. Achar and G. R. Barsch, *Phys. Rev.* **188**, 1361 (1969).
⁹H. Kaplan, *Phys. Rev.* **125**, 1271 (1962).
¹⁰W. Kress and F. W. de Wette, *Surface Phonons* (Springer, Berlin, 1991).
¹¹N. Esser, *Appl. Phys. A: Mater. Sci. Process.* **69**, 507 (1999).
¹²N. Esser, K. Hinrichs, J. R. Power, W. Richter, and J. Fritsch, *Phys. Rev. B* **66**, 075330 (2002).
¹³L. Sorba, E. Molinari, and A. Fasolino, *Surf. Sci.* **211-212**, 354 (1989).
¹⁴L. Dobrzynski, B. Djafari-Rouhani, and O. HardouinDuparc, *Phys. Rev. B* **29**, 3138 (1984).
¹⁵B. Djafari-Rouhani, J. Sapriel, and F. Bonnouvrier, *Superlattices Microstruct.* **1**, 29 (1985).
¹⁶D. W. Feldman, J. H. Parker, Jr., W. J. Choyke, and L. Patrick, *Phys. Rev.* **170**, 698 (1968).
¹⁷S. Nakashima, H. Katahama, Y. Nakakura, and A. Mitsuishi, *Phys. Rev. B* **33**, 5721 (1986).
¹⁸S. Nakashima and K. Tahara, *Phys. Rev. B* **40**, 6339 (1989).
¹⁹S. Nakashima, H. Harima, T. Tomita, and T. Suemoto, *Phys. Rev. B* **62**, 16605 (2000).
²⁰S. Zollner, J. G. Chen, E. Duda, T. Wetteroth, S. R. Wilson, and J. N. Hilfiker, *J. Appl. Phys.* **85**, 8353 (1999).
²¹T. Tomita, S. Saito, M. Baba, M. Hundhausen, T. Suemoto, and S. Nakashima, *Phys. Rev. B* **62**, 12896 (2000).
²²S. Nakashima and K. Tahara, *Phys. Rev. B* **40**, 6345 (1989).
²³A. S. Barker, Jr., J. L. Merz, and A. C. Gossard, *Phys. Rev. B* **17**, 3181 (1978).
²⁴A. Sarua, J. Monecke, G. Irmer, I. M. Triginyanu, G. Gortner, and H. L. Hartnagel, *J. Phys.: Condens. Matter* **13**, 6687 (2001).
²⁵J. Menendez and M. Cardona, *Phys. Rev. B* **31**, 3696 (1985).
²⁶W. Kauschke and M. Cardona, *Phys. Rev. B* **33**, 5473 (1986).
²⁷See, for example, M. Inoue, I. Teramoto, and S. Takayanagi, *J. Appl. Phys.* **33**, 2578 (1962).
²⁸G. Götz, A. Horstmann, E. Stein von Kaminski, and H. Kurz, *Inst. Phys. Conf. Ser.* **142**, 633 (1996).
²⁹J. L. Bischoff, D. Dentel, and L. Kubler, *Surf. Sci.* **415**, 392 (1998).